Proc. Natl. Acad. Sci. USA
Vol. 93, pp. 9510–9514, September 1996
Biochemistry

Design of artificial sequence-specific DNA bending ligands

DAVID A. LIBERLES AND PETER B. DERVAN*

Division of Chemistry and Chemical Engineering, California Institute of Technology, Pasadena, CA 91125

Contributed by Peter B. Dervan, April 15, 1996

ABSTRACT **Proteins that bend DNA are important regulators of biological processes. Sequence-specific DNA bending ligands have been designed that bind two noncontiguous sites in the major groove and induce a bend in the DNA. An oligonucleotide containing pyrimidine segments separated by a central variable linker domain simultaneously binds by triple helix formation two 15-bp purine tracts separated by 10 bp. Bend angles of 61°, 50°, and 38° directed towards the minor groove were quantitated by phasing analysis for linkers of four, five, and six T residues, respectively. The design and synthesis of nonnatural architectural factors may provide a new class of reagents for use in biology and human medicine.**

DNA bending proteins play a role in site-specific recombination, transposition, replication, viral integration, and transcription (1–12). At least three different mechanisms for protein–DNA bending have emerged. These include wedging intercalating groups into the helix (13–15), binding at two distal sites and looping the DNA around the protein (16–18), and charge neutralization at the phosphodiester backbone (19–21). These proteins are important both for locally distorting DNA at that site and for global molding of DNA conformation to promote the binding and action of distal factors. The design of nonnatural site-specific DNA bending ligands could be envisioned through one of the mechanisms used by proteins.

Oligonucleotide-directed triple helix formation is a general method for the sequence-specific recognition of double helical DNA. Two classes of triple helix forming oligonucleotides have been identified (22–26). In one class, pyrimidine oligonucleotides bind double helical DNA in the major groove parallel to the purine tract through the formation of specific Hoogsteen hydrogen bonds (22–36). Using triple helix formation for DNA recognition in the major groove, a bifunctional oligonucleotide was designed to mimic a DNA bending protein. DNA bending was accomplished by binding two distal DNA sites separated by 10 bp with oligonucleotides **1–6** containing two DNA-binding domains at the 5′ and 3′ ends connected by a variable spacer (see Fig. 1).

MATERIALS AND METHODS

General. Phosphoramidites were purchased from Glen Research (Sterling, VA) and BioGenex Laboratories (San Ramon, CA). DNA synthesis was performed using standard methods on an Applied Biosystems model 380B DNA synthesizer. Oligonucleotide purification was performed on a Pharmacia fast protein liquid chromatography using Pro-RPC reverse phase and Mono Q anion exchange columns. Enzymes were purchased from Boehringer Mannheim with the exception of Sequenase 2.0, which was purchased from United States Biochemical. Deoxyadenosine 5′-[α-^{32}P]triphosphate was obtained from Amersham. Storage Phosphor autoradiography was performed using a Molecular Dynamics model 400S Phosphorimager and IMAGEQUANT software (National Institutes of Health, Bethesda). Autoradiography used Kodak X-OMAT AR film without an intensifying screen.

Preparation of Labeled DNA. For the circular permutation assay, 101-bp 3′-end labeled restriction products were generated by digestion with the designated restriction enzyme and simultaneously filled in with Sequenase 2.0, deoxyadenosine 5′-[α-^{32}P]triphosphate, and nonradioactive deoxynucleoside triphosphates. The 101-bp fragment was isolated by nondenaturing 5% PAGE and the purified fragment was treated with proteinase K, filtered, further extracted with phenol/chloroform, and precipitated with ethanol. The 577–585-bp fragments for phasing assays were generated by cleavage of pUC19 derived plasmids with *Nde*I and *Sap*I (New England Biolabs) and purified as above.

Quantitative DNase I Footprint Titrations. The binding energy was calculated from the equilibrium association constants of the oligonucleotides 5′-T$\underline{C}$T$\underline{C}$T$\underline{C}\underline{C}T\underline{C}\underline{C}T\underline{C}T\underline{C}$T-3′ and 5′-T$\underline{C}\underline{C}T\underline{C}T\underline{C}T\underline{C}T\underline{C}T\underline{C}\underline{C}$T-3′ (where $\underline{C}$ is 5-methyl cytosine) binding to their cognate sites by quantitative DNase I footprint titrations. The values reported are the mean value of four footprint titration experiments ± SEM. Oligonucleotide titrations were performed at 22°C, pH 5.5, in the presence of 45 mM Mes, 1 mM $MgCl_2$, and ^{32}P-3′-end-labeled target DNA and allowed to equilibrate for at least 24 hr before footprinting. Footprinting reactions and data analysis were carried out as described (27, 37).

Gel-Shift Assay. The gel-shift assay was performed by equilibrating samples for at least 1 hr at 22°C, pH 5.5, with 10 μM oligonucleotide, 45 mM Mes, 1 mM $MgCl_2$, and ^{32}P-3′-end-labeled *Eco*RI cut target DNA in a vol of 10 μl. One microliter of 15% glycerol loading buffer was then added. Samples were run on a 10% polyacrylamide gel at 4°C, pH 5.5, with a 75:1 acrylamide/bis-acrylamide ratio in 45 mM Mes and 1 mM $MgCl_2$ with buffer recirculation.

Circular Permutation Analysis. Circular permutation analysis was performed under similar gel-shift conditions. Experiments were performed with equilibrations at 22°C, pH 5.5, with 45 mM Mes and 1 mM $MgCl_2$ containing 20 μM oligonucleotide.

Phasing Analysis. Phasing analysis was performed on 577–585-bp fragments where the intrinisically curved sequence 5′-AAAAAACGGCAAAAAACGGGCAAAAAA-3′ was linked by a variable G+C tract to the target sequence. Equilibrations were performed as in the gel-shift assay with an oligonucleotide concentration of 10 μM under similar electrophoretic conditions with a 7% polyacrylamide gel and a 32:1 acrylamide/bis-acrylamide ratio.

Quantitation of Bend Angle. Bend angle quantitation was based on previously described methods (21, 38–40). Briefly, the relationship between the distance migrated and fragment size for molecular weight standards was plotted and fit to a logarithmic function (41). This was used to determine the relative mobilities of the various bent fragments, which were plotted and fit to the cosine function $\mu = \mu_{ave}\{A_{ph}/2[\cos(2\pi(S-S_T/P_{ph}))] + 1\}$, where μ is the electrophoretic

The publication costs of this article were defrayed in part by page charge payment. This article must therefore be hereby marked "*advertisement*" in accordance with 18 U.S.C. §1734 solely to indicate this fact.

*To whom reprint requests should be addressed.

mobility measured in apparent base pairs (R_L), A_{ph} is the phasing amplitude, S is the distance between bend centers, S_T is the out of phase bend center distance, and P_{ph} is the phasing period (21, 40). The bend angle, α_B, was then determined from the geometrically derived phasing function $\tan(k\alpha_B/2) = (A_{ph}/2)/\tan(k\alpha_C/2)$ where α_C is the A tract bend angle (21, 40). A standardization value, k, for electrophoretic conditions was calculated to be 1.20 ± 0.11 using fragments that were retarded only by the inserted A tract (21, 40). The fragment, in addition to the inserted A tract, was found to have an intrinsic curvature of 18° ± 0.4°, which was 2.3 ± 0.1 bp out of phase with the target site. The additional intrinsic fragment bend angle in the same plane was subtracted from the obtained angle to yield the bend angle of the structure.

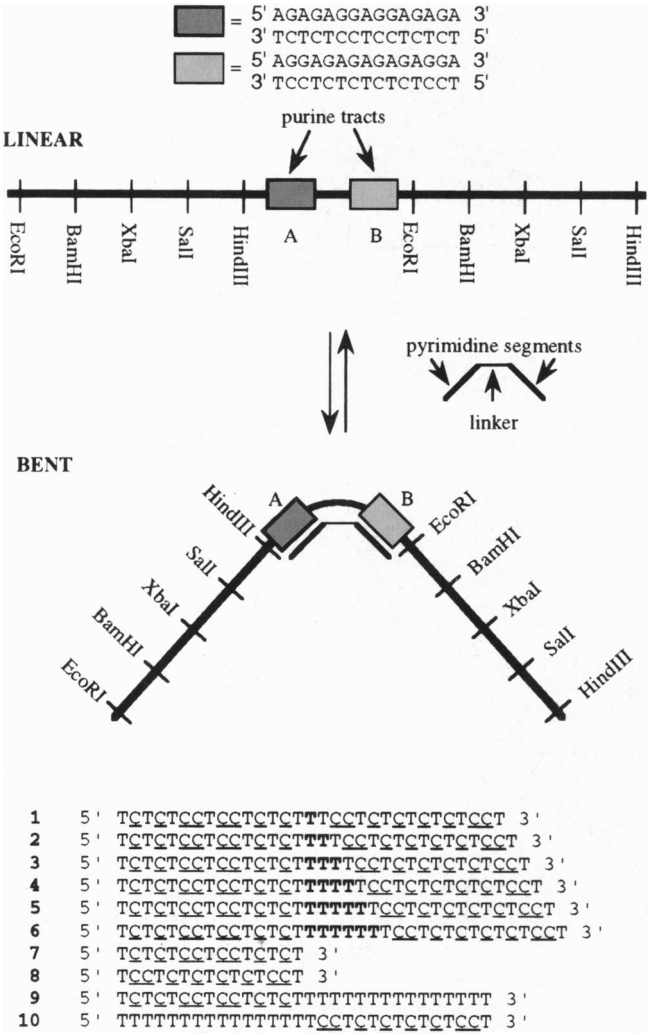

FIG. 1. Circular permutation analysis of ligand induced bending. The 101-bp probes used for circular permutation analysis were generated by restriction enzyme cleavage at sites within tandem polylinkers surrounding the ligand binding site. The plasmid contains the sequence 5′-GAATTCGAGCTCGGTACCCGGGGATCCTCTAGAGTCGACCTGCAGGCATGCAAGCTT**AGAGAGGAGGAGAGAGCGGTGCGGTAGGAGAGAGAGAG**GAGAATTCGAGCTCGGTACCCGGGGATCCTCTAGAGTCGACCTGCAGGCATGCAAGCTT-3′. The ligands designed to bend DNA sequence specifically were two third strand oligonucleotide domains containing 5-methyl C (indicated by C) and T residues linked by a variable number of T residues.

RESULTS AND DISCUSSION

Two 15-bp purine tracts separated by one turn of the DNA helix (10 bp) were targeted by oligonucleotides **1–6** containing two pyrimidine tracts (T and ^{Me}C) connected by a central T linker of varying size. Previous studies have demonstrated that nonadjacent purine tracts can be bound simultaneously, but the influence of oligonucleotide length and sequence composition on bend angle was not examined (42, 43). To allow bending of DNA, the binding energies of the two third strand oligonucleotides must be greater than the energetic penalty for bending. The equilibrium association constant, K_{eq}, of 15-mer oligonucleotide **7**, 5′-T^{Me}CT^{Me}CT^{Me}C^{Me}CT^{Me}C^{Me}CT^{Me}CT^{Me}CT-3′ (targeted to site A) was measured as $K_{eq} = 2.2 \pm 0.2 \times 10^7$ M^{-1}, while that for 15-mer oligonucleotide **8**, 5′-T^{Me}C^{Me}CT^{Me}CT^{Me}CT^{Me}CT^{Me}CT^{Me}C^{Me}CT-3′ (targeted to site B) was measured as $K_{eq} = 1.7 \pm 0.1 \times 10^7$ M^{-1} by quantitative DNase I footprint titration methods at 22°C and pH 5.5 (Fig. 1). From these equilibrium association constants, the binding energies of oligonucleotides bound at site A and site B were calculated as −10.0 ± 0.1 kcal/mol and −9.9 ± 0.1 kcal/mol, respectively.

DNA bending as a function of linker size was initially screened using a circular permutation assay (44). This assay is based upon the theory that DNA mobility is directly related to the mean square end-to-end distance for fragments of the same size (45). A bending target site was cloned between tandem polylinkers into pUC19. Cleavage with various restriction enzymes gave a series of 101-bp fragments in which the target site is located at various positions. As the bend site is moved through the fragment, the end-to-end distance changes.

The sequence specific binding ligands can bind as one oligonucleotide bound to two sites (bent), one oligonucleotide bound to one site (Y), or as two oligonucleotides bound to two sites (double Y). Control oligonucleotides **9** and **10** contain a mismatch in one of the triplex sites and only bind to one of the two designated target sites. Oligonucleotide **4**, which contains two pyrimidine tracts separated by a central T_4 linker, reveals

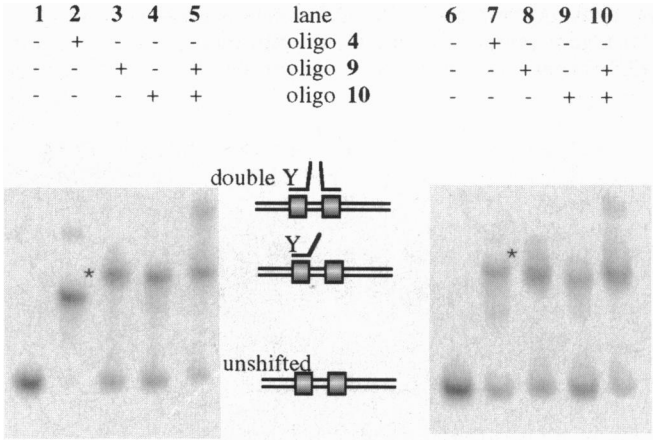

FIG. 2. PhosphorImage using a linear dynamic range of 50 of a 10% (75:1 acrylamide/bis ratio) polyacrylamide gel run in 45 mM Mes, 1 mM $MgCl_2$, pH 5.5 at 4°C showing a gel-shift analysis of oligonucleotides **4**, **9**, and **10**. The *Eco*RI and *Xba*I fragments from Fig. 1, with the triple helix target sites near the termini and near the center, respectively, were generated and 3′-end-labeled with ^{32}P. Oligonucleotides were incubated at a concentration of 5 μM at 22°C at pH 5.5, with 45 mM Mes and 1 mM $MgCl_2$. Lanes 1 and 6 show the *Eco*RI and *Xba*I fragments, respectively, incubated without oligonucleotide. Lanes 2 and 7 show the gel-shift generated by oligonucleotide **4**, with the bent fragment indicated by an asterisk. Lanes 3 and 8 depict this for oligonucleotide **9**, lanes 4 and 9 for oligonucleotide **10**, and lanes 5 and 10 for an incubation with both oligonucleotides **9** and **10**.

that it is not bound as a Y or as a double Y (Fig. 2). Addition of control oligonucleotides **9** and **10** affords both the Y and double Y structures. In addition, mobilities of the Y and double Y structures are unchanged between the *Eco*RI and *Xba*I fragments shown on both sides of Fig. 2, indicating no induced DNA bend.

Circular permutation analysis of the bent structures shows significant position-dependent anomalous mobility as a function of linker length. Oligonucleotides with shorter linkers yield larger bend angles (Fig. 3). A three T spacer appears to be the minimal linker where a majority of the molecular ensemble is in the bent conformation under these conditions. As the linker size is further shortened, a decreasing proportion of the molecular ensemble is found as the bent structure with a concomitant increase in the populations of Y and double Y species. A range of bend angles of differing magnitude can be produced and the linker size can be tuned to yield the magnitude of the desired bend angle.

The circular permutation assay has been found to overestimate bend angles where other factors such as increased DNA flexibility or binding of a ligand that is large compared with the target duplex affect migration (21, 46). While such complicating effects are not anticipated in this experimental design, a phasing analysis was used to measure the bend angles of oligonucleotides **4–6** (Fig. 4*A*) (38). The A tract used in this experiment has a bend angle of 54° and oligonucleotides **4–6** were found to provide bend angles of 61° ± 2.7°, 50° ± 1.0°, and 38° ± 0.5°, respectively (Fig. 4 *B* and *C* and Table 1) (47). Phasing analysis also provides information on bend direction. The bend was found to be centered in the middle of the intervening duplex directed towards the minor groove.

To form the bent structure, the third strand oligonucleotide most likely binds initially at a single site. The DNA then must show sufficient dynamic flexibility to allow binding of the second domain. The final structure obtained is a function of the energetic difference between the binding energy of the third strand and the requisite bending energy caused by constriction of the DNA. The thermodynamically favored structure occurs where this difference is greatest, with other structures populated dependent upon their relative energetic differences. The energetic cost of bending DNA can be

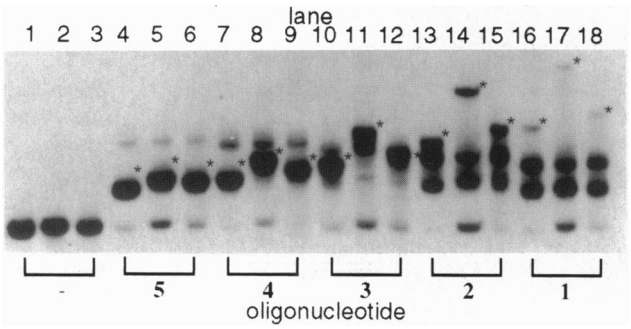

FIG. 3. Autoradiogram of a 10% (75:1 acrylamide/bis ratio) polyacrylamide gel run in 45 mM Mes and 1 mM $MgCl_2$ at pH 5.5 and at 4°C showing circular permutation analysis of bending using oligonucleotides **1–5**. *Eco*RI, *Xba*I, and *Hin*dIII fragments from Fig. 1 were generated and 3′-end-labeled with ^{32}P. Oligonucleotides were incubated at a concentration of 20 μM at 22°C, with 45 mM Mes and 1 mM $MgCl_2$ at pH 5.5. Lanes 1–3 show the *Eco*RI, *Xba*I, and *Hin*dIII fragments, respectively, incubated without oligonucleotide. Lanes 4–6 show oligonucleotide **5** incubated with the *Eco*RI, *Xba*I, and *Hin*dIII fragments, respectively. Lanes 7–9 depict oligonucleotide **4** binding to the three fragments, respectively, while lanes 10–12 depict this for oligonucleotide **3**, lanes 13–15 depict this for oligonucleotide **2**, and lanes 16–18 depict this for oligonucleotide **1**. Bent fragments are indicated with an asterisk.

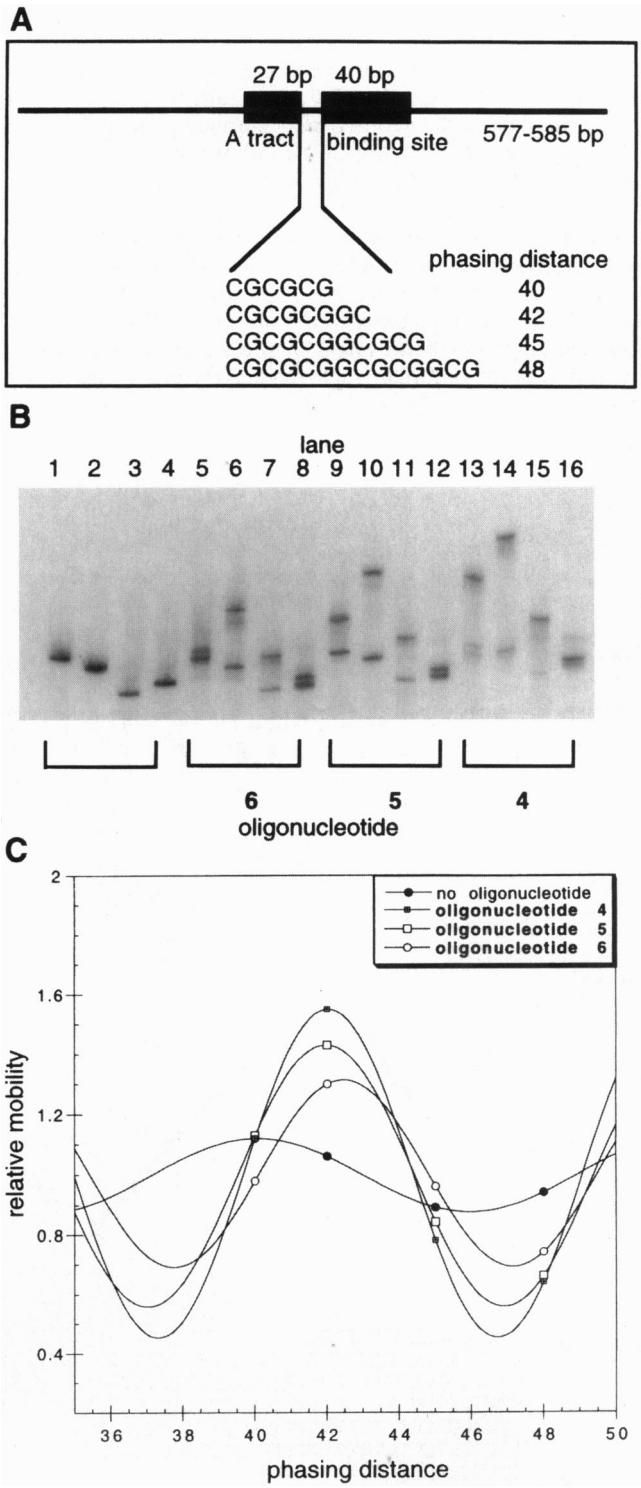

FIG. 4. (*A*) General schematic for phasing analysis of DNA bending. A set of three phased A_6 tracts with total bend angle of 54° is separated by the phasing distance from a second bend. (*B*) Autoradiogram of a 7% (32:1 acrylamide/bis ratio) polyacrylamide gel run in 45 mM Mes and, 1 mM $MgCl_2$ at pH 5.5 and at 4°C showing phasing analysis of bending oligonucleotides **4–6**. The 577–585-bp fragments generated by simultaneous *Sap*I/*Nde*I cleavage were 3′-end-labeled with ^{32}P. Oligonucleotides were incubated at a concentration of 10 μM at 22°C and at pH 5.5 with 45 mM Mes and 1 mM $MgCl_2$. Lanes 1–4 depict the four phasing fragments with phasing distances of 40, 42, 45, and 48 respectively with no oligonucleotide present while lanes 5–8 depict the respective fragments with oligonucleotide **6** bound, lanes 9–12 with oligonucleotide **5** bound, and lanes 13–16 with oligonucleotide **4** bound. (*C*) Phasing diagram for oligonucleotides **4–6**. The mobilities of these oligonucleotides were plotted against the phasing distance and fit to a standard cosine function (21).

Table 1. Bend angles measured by phasing analysis for triple helical structures with variable linker sizes at pH 5.5 with oligonucleotides containing 5-methyl C and T

Oligonucleotide	Linker size	Bend angle
4	4	61° ± 2.7°
5	5	50° ± 1.0°
6	6	38° ± 0.5°

Error values reported are the standard error of the mean. The error limits on the bend angles likely do not reflect the semiquantitative nature of the analysis and should be considered minimum values.

estimated by modeling DNA as a smoothly bending worm-like chain with coulombic repulsion from phosphates placed at fixed distances (48, 49). Assuming the third strand is fully hydrogen bonded and ignoring cooperative effects, this model predicts a bend angle of 86° to promote equal ratios of bent and straight DNA for an oligonucleotide with a calculated binding energy of −9.9 kcal/mole. Circular permutation analysis reveals a single bent structure that decreases in population as the linker length decreases but remains populated at a length of a single T residue (Fig. 3). For a linker of three T residues, the ratio of bent to straight DNA is approximately one. The bend angle of this structure was too high to measure accurately using phasing analysis and a four T linker was the smallest that was characterized quantitatively, with a bend angle of 61°. A ribbon model that depicts a bent structure with a four base linker is shown in Fig. 5. This model is bent towards the minor groove at the center of the intervening duplex, with the four T linker of the third strand pulled taut away from the duplex and unstacked.

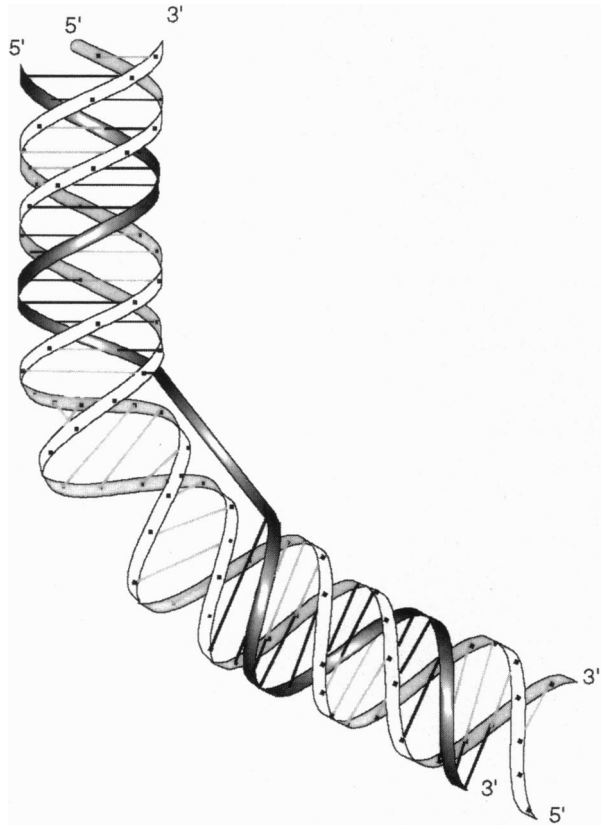

FIG. 5. Ribbon model of bent structure formed by oligonucleotide **4**. Two 15-bp triple helices are connected by a four T linker spanning the intervening 10 bp of double helix. This region is bent towards the minor groove in the center.

We are grateful for support from the National Institutes of Health (Grant GM 51747).

1. Thompson, J. F. & Landy, A. (1988) *Nucleic Acids Res.* **16,** 9687–9705.
2. Goodman, S. D., Nicholson, S. C. & Nash, H. A. (1992) *Proc. Natl. Acad. Sci. USA* **89,** 11910–11914.
3. Hallet, B., Rezsohazy, R., Mahillon, J. & Delcour, J. (1994) *Mol. Microbiol.* **14,** 131–139.
4. Goryshin, I. Y., Kil, Y. V. & Reznikoff, W. S. (1994) *Proc. Natl. Acad. Sci. USA* **91,** 10834–10838.
5. Henriquez, V., Milisavljevic, V., Kahn, J. D. & Gennaro, M. L. (1993) *Gene* **134,** 93–98.
6. Nakajima, M., Sheikh, Q. I., Yamaoka, K., Yui, Y., Kajiwara, S. & Shishido, K. (1993) *Mol. Gen. Genet.* **237,** 1–9.
7. Muller, H. P. & Varmus, H. E. (1994) *EMBO J.* **13,** 4704–4714.
8. Milot, E., Belmaaza, A., Rassart, E. & Chartrand, P. (1994) *Virology* **201,** 408–412.
9. Natesan, S. & Gilman, M. Z. (1993) *Genes Dev.* **7,** 2497–2509.
10. Meacock, S., Pescini-Gobert, R., DeLamarter, J. F. & van Huijsduijen, R. H. (1994) *J. Biol. Chem.* **269,** 31756–31762.
11. Kim, J., Klooster, S. & Shapiro, D. J. (1995) *J. Biol. Chem.* **270,** 1282–1288.
12. Perez-Martin, J., Rojo, F. & DeLorenzo, V. (1994) *Microbiol. Rev.* **58,** 268–290.
13. Kim, J. L., Nikolov, D. B. & Burley, S. K. (1993) *Nature (London)* **365,** 520–527.
14. Kim, Y., Geiger, J. H., Hahn, S. & Sigler, P. B. (1993) *Nature (London)* **365,** 512–520.
15. Haqq, C. M., King, C., Ukiyama, E., Falsafi, S., Haqq, T. N., Donahoe, P. K. & Weiss, M. A. (1994) *Science* **266,** 1494–1500.
16. Mondragon, A. & Harrison, S. C. (1991) *J. Mol. Biol.* **219,** 321–334.
17. Fisher, R. F. & Long, S. R. (1993) *J. Mol. Biol.* **233,** 336–348.
18. Finzi, L. & Gelles, J. (1995) *Science* **267,** 378–380.
19. Manning, G. S., Ebralidse, K. K., Mirzabekov, A. D. & Rich, A. (1989) *J. Biomol. Struct. Dyn.* **6,** 877–889.
20. Strauss, J. K. & Maher, L. J. (1994) *Science* **266,** 1829–1834.
21. Kerppola, T. K. & Curran, T. (1991) *Science* **256,** 1210–1214.
22. Moser, H. & Dervan, P. B. (1987) *Science* **238,** 645–650.
23. LeDoan, T., Perrouault, L., Praseuth, D., Habhoub, N., Decout, J., Thuong, N. T., Lhomme, J. & Helene, C. (1987) *Nucleic Acids Res.* **15,** 7749–7760.
24. Cooney, M., Czernuszewicz, G., Postel, E. H., Flint, S. J. & Hogan, M. E. (1988) *Science* **241,** 456–459.
25. Beal, P. A. & Dervan, P. B. (1991) *Science* **251,** 1360–1363.
26. Beal, P. A. & Dervan, P. B. (1992) *Nucleic Acids Res.* **20,** 2773–2776.
27. Singleton, S. F. & Dervan, P. B. (1992) *J. Am. Chem. Soc.* **114,** 6957–6965.
28. Roberts, R. W. & Crothers, D. M. (1991) *Proc. Natl. Acad. Sci. USA* **88,** 9397–9401.
29. Rougee, M., Faucon, B., Mergny, J. L., Barcelo, F., Giovannageli, C., Garestier, T. & Helene, C. (1992) *Biochemistry* **31,** 9269–9278.
30. Fossella, J. A., Kim, Y. J., Shih, H., Richards, E. G. & Fresco, J. R. (1993) *Nucleic Acids Res.* **21,** 4511–4515.
31. Best, G. C. & Dervan, P. B. (1995) *J. Am. Chem. Soc.* **117,** 1187–1193.
32. Povsic, T. J. & Dervan, P. B. (1989) *J. Am. Chem. Soc.* **111,** 3059–3061.
33. Xodo, L. E., Manzini, G., Quadrifoglio, F., van der Marel, G. A. & van Boom, J. H. (1991) *Nucleic Acids Res.* **19,** 5625–5631.
34. Singleton, S. F. & Dervan, P. B. (1992) *Biochemistry* **31,** 10995–11003.
35. Singleton, S. F. & Dervan, P. B. (1993) *Biochemistry* **32,** 13171–13179.
36. Singleton, S. F. & Dervan, P. B. (1994) *J. Am. Chem. Soc.* **116,** 10376–10382.
37. Brenowitz, M., Senear, D. F., Shea, M. A. & Ackers, G. K. (1986) *Proc. Natl. Acad. Sci. USA* **83,** 8462–8466.
38. Zinkel, S. S. & Crothers, D. M. (1987) *Nature (London)* **328,** 178–181.
39. Zinkel, S. S. & Crothers, D. M. (1990) *Biopolymers* **29,** 29–38.
40. Kerppola, T. K. & Curran, T. (1993) *Mol. Cell. Biol.* **13,** 5479–5489.

41. Maniatis, T., Jeffrey, A. & van deSande, H. (1975) *Biochemistry* **14,** 3787–3794.
42. Kessler, D. J., Pettitt, B. M., Cheng, Y., Smith, S. R., Jayaraman, K., Vu, H. M. & Hogan, M. E. (1993) *Nucleic Acids Res.* **21,** 4810–4815.
43. Kiyama, R. & Oishi, M. (1995) *Nucleic Acids Res.* **23,** 452–458.
44. Wu, H. & Crothers, D. M. (1984) *Nature (London)* **308,** 509–513.
45. Zimm, B. H. & Levene, S. D. (1992) *Q. Rev. Biophys.* **25,** 171–204.
46. Kuprash, D. V., Rice, N. R. & Nedospasov, S. A. (1995) *Nucleic Acids Res.* **23,** 427–433.
47. Koo, H., Drak, J., Rice, J. A. & Crothers, D. M. (1990) *Biochemistry* **29,** 4227–4234.
48. Bloomfield, V. A., Crothers, D. M. & Tinoco, I. (1974) *Physical Chemistry of Nucleic Acids* (Harper and Row, New York), pp. 159–166.
49. Fenley, M. O., Manning, G. S. & Olson, W. K. (1992) *J. Phys. Chem.* **96,** 3963–3969.